

Methanol Synthesis over Cu/ZnO/Al₂O₃: The Active Site in Industrial Catalysis

Malte Behrens,^{*,a} Felix Studt,^{*,b} Igor Kasatkin,^a Stefanie Kühl,^a Michael Hävecker,^c Frank Abild-Pedersen,^b Stefan Zander,^a Frank Girgsdies,^a Patrick Kurr,^d Michael Tovar,^e Richard W. Fischer,^d Jens K. Nørskov,^{b,e} R. Schlögl^a

^a Fritz Haber Institute of the Max Planck Society, Department of Inorganic Chemistry, Faradayweg 4-6, 14195 Berlin, Germany

^b SUNCAT Center for Interface Science and Catalysis, SLAC National Accelerator Laboratory, 2575 Sand Hill Road, Menlo Park, California 94025, USA

^c Division Solar Energy Research, Elektronenspeicherring BESSY II, Helmholtz-Zentrum Berlin für Materialien und Energie, Albert-Einstein-Str. 15, 12489 Berlin, Germany

^d Süd-Chemie AG, Research & Development Catalysis & Energy, Waldheimer Straße 13, 83052 Bruckmühl, Germany.

^d Institute for Complex Magnetic Materials, Helmholtz-Zentrum Berlin für Materialien und Energie, Hahn-Meitner-Platz 1, 14109 Berlin, Germany

^e Department of Chemical Engineering, Stanford University, Stanford, California 94305, USA

* behrens@fhi-berlin.mpg.de, studt@slac.stanford.edu

Unlike homogeneous catalysts, heterogeneous catalysts that have been optimized through decades are typically so complex and hard to characterize that the nature of the catalytically active site is not known. This is one of the main stumbling blocks in developing rational catalyst design strategies in heterogeneous catalysis. We show here how to identify the crucial atomic structure motif for the industrial Cu/ZnO/Al₂O₃ methanol synthesis catalyst. Using a combination of experimental evidence from bulk-, surface-sensitive and imaging methods collected on real high-performance catalytic systems in combination with DFT calculations. We show that the active site consists of Cu steps peppered with Zn atoms, all stabilized by a series of well defined bulk defects and surface species that need jointly to be present for the system to work.

Methanol is an important feedstock in chemical industries for many value-added products. It is industrially produced from synthesis gas mixtures (H₂/CO₂/CO) at elevated pressures and temperatures ($p = 50 - 100$ bar, $T = 200 - 300$ °C) over Cu/ZnO/Al₂O₃ catalysts with a worldwide demand of ca. 47 Mt year⁻¹ (2010).¹ Furthermore, recent interest in this catalytic system is due to the potential of methanol as a sustainable synthetic fuel, which can be obtained by hydrogenation of the greenhouse gas CO₂.² Due to the enormous economic relevance of the methanol synthesis reaction, the phenomenological optimization of the preparation of catalytically very active “methanol copper” is far more advanced than the fundamental understanding of its high catalytic activity. The nature of the active site on Cu/ZnO-based high-performance catalysts for methanol synthesis has been vividly debated in literature³ and is still not comprehensively understood.

Industrially applied Cu/ZnO-based catalysts are prepared by a co-precipitation method developed in industry in the 1960s,^{4,5} which leads to formation of porous aggregates of Cu and ZnO nanoparticles.⁶ To form this unique microstructure, Cu-rich molar compositions of Cu:Zn near 70:30 have to be

Submitted to Science

Work supported in part by US Department of Energy contract DE-AC02-76SF00515.

applied.⁷ Thus, the industrial system is a bulk catalyst, which is characterized by a high Cu:Zn ratio with > 50 mol% Cu (metal base), approximately spherical Cu nanoparticles of a size around 10 nm and ZnO particles, which are arranged in an alternating fashion to form porous aggregates. These aggregates expose a large Cu surface area of up to ca. 40 m²g⁻¹. Furthermore, industrial catalysts contain low amounts of a refractory oxide as structural promoter,⁸ in most cases up to ca. 10 % Al₂O₃. Omitting any of the constituting elements drastically reduces the performance of the system.

One important key to high performance is a large accessible Cu surface area,⁹ which has been observed to scale linearly with the activity for sample families with a similar preparation history.¹⁰ However, between these families considerably different intrinsic activities, i.e. activities normalized by the Cu surface area, can be found. Thus, different “qualities” of Cu surfaces can be prepared, which vary in the activity of their active sites and/or in the concentration of these sites. Hence, methanol synthesis over Cu appears to be a structure sensitive reaction.¹¹⁻¹³

One important function of ZnO certainly is that it helps to effectively disperse the Cu phase in course of catalyst preparation⁷ and is thus responsible for the high Cu surface areas of industrial catalysts. However, it has been since long recognized that the role of ZnO in the final composite catalyst goes beyond that of a mere physical spacer between Cu nanoparticles preventing them from sintering. The presence of ZnO beneficially affects the intrinsic activity of Cu-based methanol synthesis catalysts, which is known as the Cu-ZnO synergy.¹⁴⁻¹⁶ Over the past decades of Cu/ZnO research, many different models have been proposed to explain this synergistic effect.¹⁷⁻²⁴ This undissolved controversy is partially because in some cases the experimental evidence could not be obtained on the highly optimized and mature technical system, but rather on simplified model samples ranging from Cu single crystals to Cu nanoparticles supported on highly crystalline ZnO with a low loading, thus, with a composition and microstructure strongly deviating from that of the industrial catalyst described above.

Investigations on industrial samples and other co-precipitated systems have suggested that defects⁶ and lattice strain²⁵ in the Cu particles affects the intrinsic activity of the Cu surface. To study the role of defects in the real Cu/ZnO/(Al₂O₃) composite system, we have prepared a series of five functional catalysts and compared them to a pure Cu metal reference sample. Details on the different samples can be found as supporting information. It is noted that all samples are characterized by a high Cu loading of at least 50 mol% (metal base), Cu particle sizes of between 5 and 15 nm and exposed Cu surface areas of 10 m²g⁻¹ or higher. These properties make them similar to the industrially applied material. In order to allow for a reliable correlation of catalytic and structural data, the microstructural homogeneity of the prepared catalysts has been carefully checked. Samples have been prepared from close-to single phase precursor materials resulting in relatively homogeneous element distributions and mono-modal Cu particle size distributions after thermal treatment. The catalytic activity of all six samples was measured under industrial conditions at p = 60 bar and T = 210 °C and 250 °C in a typical syngas mixture (for details see supporting information). The results are shown together with the Cu surface areas in Figure 1a. The ZnO-free Cu reference shows no significant activity, while those catalysts perform best, which have been prepared following the industrial recipe. Methanol was produced by all five catalysts, which cover a wide range of activities. Normalizing the performances to that of the most active catalyst (at both temperatures) and dividing by the Cu surface areas result in the intrinsic activities shown in Figure 1b. The scattering of the data shows that the Cu surface area alone cannot explain the differences in performance

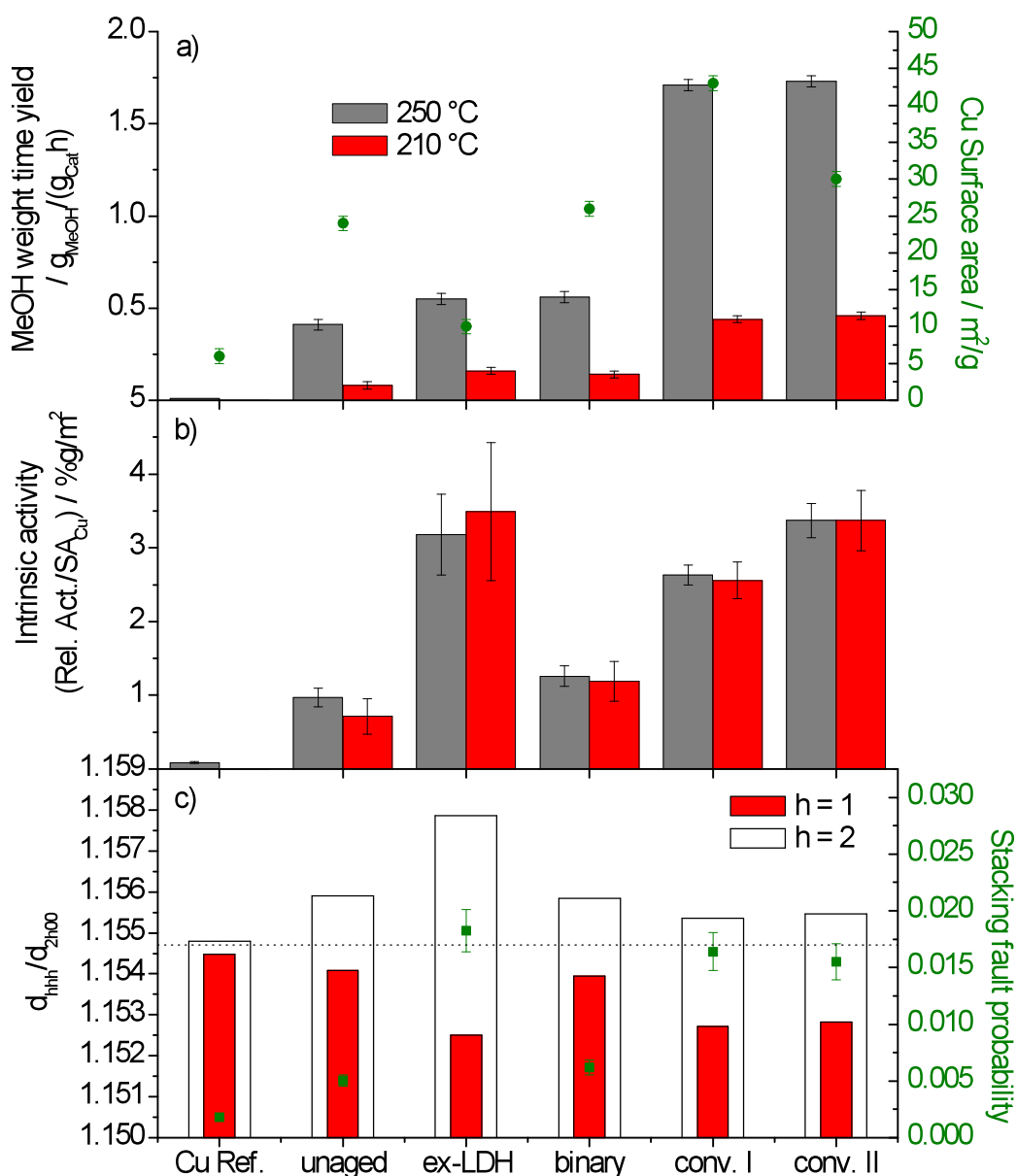


Figure 1: a) Catalytic activities and Cu surface areas of the Cu reference material and the five Cu/ZnO/Al₂O₃ catalysts in methanol synthesis ($p = 60$ bars, $T = 210, 250$ °C). b) Intrinsic activities per Cu surface area obtained after normalization (most active sample = 100% at both temperatures). c) Deviation of d_{111}/d_{200} and d_{222}/d_{400} observed in the neutron diffraction patterns and resulting stacking fault probabilities of the Cu particles. For a detailed description of the samples and explanation of sample labeling see supporting information.

To find a structural explanation for the observed trend, neutron diffraction experiments were done on the reduced catalysts. Broad peaks of the metallic Cu fcc phase indicative of small crystallite domains (3.8 – 9.9 nm) were present in all catalyst samples. The inactive pure Cu reference samples exhibited larger domains of > 100 nm and better developed peaks. An analysis of the planar defect structure was performed using a pattern decomposition method. It is well-known that characteristic diffraction peaks will broaden and shift from their ideal position as a function of increased stacking fault concentration.²⁶ The shift of the 111 and 200 peaks towards each other and the simultaneous shift of the higher order peaks 222 and 400 away from each other are especially characteristic. With

the neutron data, sufficiently reliable fitting of the 400 peak position of the nanostructured Cu phase was possible. The ratios $d_{hhh}/d_{(2h)00}$ for $h = 1, 2$, which are expected to be constant at 1.1547 for an ideal fcc structure, are shown in Figure 1c. While for the inactive pure Cu sample both ratios fall near the expected ideal value, the catalytically active materials show a lower value for $h = 1$ and a higher one for $h = 2$, which is a clear qualitative proof for the presence of stacking faults in the Cu particles. For quantification the spacing of the more intensive 111 and 200 peaks was used²⁷ (Figure 1c) and the resulting stacking fault density is shown in Figure 2 to scale monotonously with the intrinsic activity. This result confirms that highly active “methanol copper” is a defective form of nanoparticulate Cu, which is rich in planar defects like stacking faults. The high abundance of defects in the active materials is tentatively related to the confined crystallization of the Cu particles in strong interfacial contact to the ZnO component during the mild catalyst activation procedure leading to a kinetically trapped form of Cu.

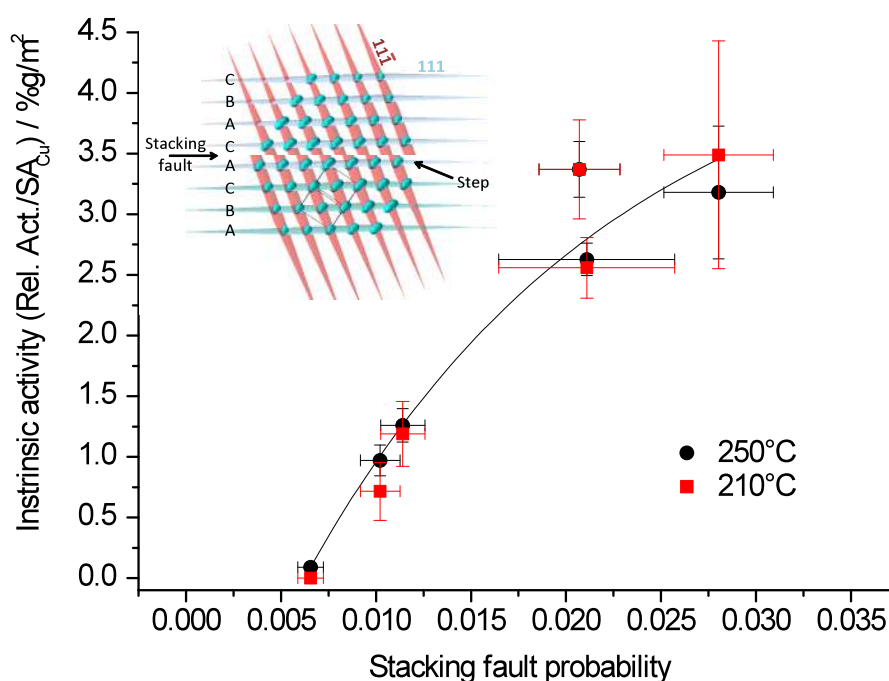


Figure 2: Relation of the intrinsic activity of Cu with the concentration of stacking faults. The line is a guide to the eye. The inset shows schematically how a stacking fault in 111 can generate a surface step in the 111 facet.

The non-ideal nature of active Cu is also manifested as strain, small coherently scattering domains and disorder. Planer defects will contribute to these properties and their general importance for Cu/ZnO catalysts has been highlighted before.^{6,25} Accordingly, we find in our series of samples also coarse trends of the intrinsic activity with a lower crystallite domain size, higher lattice strain and higher disorder. These trends were obtained independently from the stacking fault analysis by Rietveld refinement (see supporting information). The role of bulk defects for catalysis can be explained with the high probability that an extended defect terminates at the exposed surface of the Cu particle in a nanostructured system creating a line at the surface of the particle, which is higher in surface energy compared to ideally ordered terraces. It is shown schematically in the inset of Figure

2, how a stacking fault in 111 creates a step on the 111 surface of a Cu crystallite. A twin boundary terminating at a surface is associated with a kink.

The effect of steps at the Cu surface on the catalytic properties is also confirmed by density functional theory calculations on different Cu surfaces. We studied methanol formation from both, CO_2 and CO^{28} over flat Cu(111) and stepped Cu(211) surfaces (Figure 3, black and blue curves). Figure 3b shows the CO_2 hydrogenation pathway on the two different surfaces. For clarity, only the lowest energy pathway is shown, which is the same for both surfaces. Energetics of the other intermediates are given in the supporting information. Hydrogenation of CO_2 proceeds via formation of HCOO^* , HCOOH , and H_2COOH . The C-O bond of H_2COOH is split to yield adsorbed H_2CO and OH^* , where H_2CO is hydrogenated to methanol via the methoxy (CH_3O) intermediate. Surface OH is removed as water. A similar pathway for CO_2 hydrogenation on the 111 surface of Cu has been suggested in the literature recently.²⁹ Other theoretical studies have been dealing with Cu(100),³⁰ small Cu clusters³¹ or Zn atoms deposited on Cu(111).³²

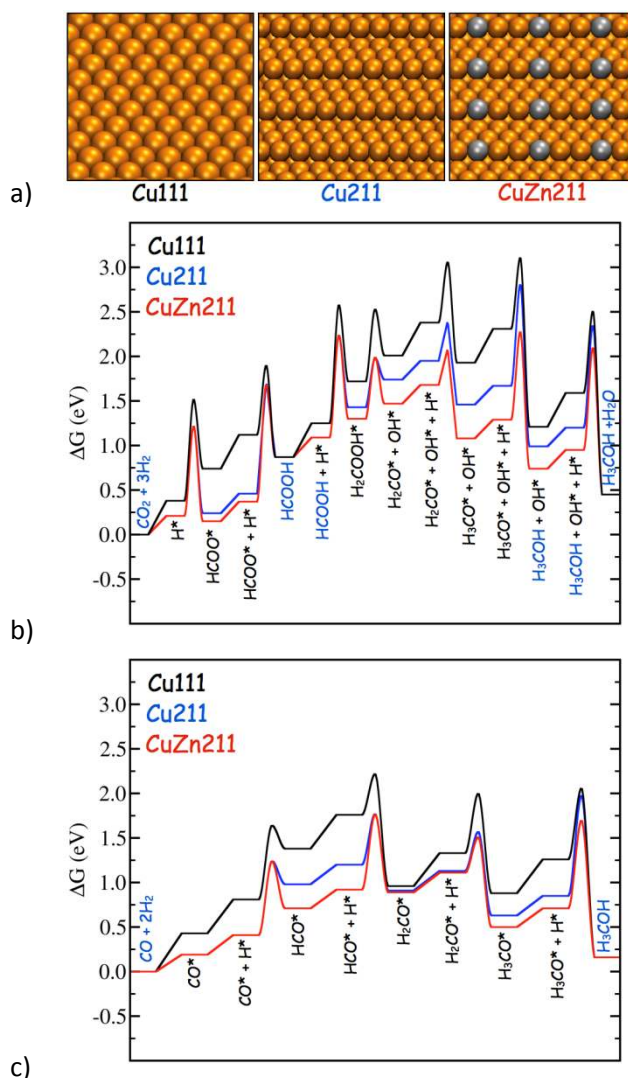


Figure 3: The Cu(111), Cu(211) and CuZn(211) facets as viewed from perspective (a). Gibbs free energy diagram obtained from DFT calculations for CO_2 (b) and CO (c) hydrogenation on close-packed (black), stepped (blue) and Zn substituted steps (red). Zn substitution was modeled by replacing one of the three Cu atoms of the step with Zn. All energies are relative to $\text{CO}_2 + 3\text{H}_2$ ($\text{CO} + 2\text{H}_2$) in the gas-

phase and the clean surfaces. Intermediates marked with a star are adsorbed on the surface. Gibbs free energies were calculated at $T = 500\text{ K}$.

As shown in Figure 3b, the flat Cu(111) surface binds weaker to the intermediates than Cu(211). Essentially all intermediates are thermodynamically less stable than CO_2 and H_2 in the gas-phase. Note that these thermodynamics do not include effects of pressure. High CO_2 and H_2 pressure will strengthen adsorption energies and make formation of methanol and water downhill in energy, explaining why high pressures are needed for this process. Both, the energies of the intermediates and the transition-state energies decrease considerably when going from the 111 to the 211 surface, rendering the steps more active than the terraces. A similar picture is obtained if hydrogenation of CO to methanol is considered (Figure 3c). CO hydrogenation proceeds via hydrogenation of the carbon end of CO with the intermediates being HCO, H_2CO , and H_3CO . H_3CO is then hydrogenated to methanol. The last two intermediates are the same as for the hydrogenation of CO_2 . It can be seen that steps again lower the adsorption energies of the intermediates significantly compared to the flat surface.

While the stepped Cu(211) surface or the stacking fault-created step shown in the inset of Figure 2 can be regarded as model situations, the relation of bulk defects and surface steps in the most active catalyst was studied with aberration-corrected high resolution transition electron microscopy (HRTEM). The vast majority of the investigated Cu nanoparticles were found to be faulted exhibiting planar extended defects, stacking faults and twin boundaries, running through the whole particle. It can be seen in Figure 4 that the particle shape can be generally approximated by a sphere. Due to the curvature of the particle, the surface intrinsically holds a number of steps. The HRTEM image 4a shows stepped surface facets like 211 and 522 being responsible for the curvature at the lower exposed side of the Cu nanoparticle. It can be seen that the surface faceting additionally changes along the line where the twin boundary terminates at the surface. This kind of kink is associated with an inward curvature of the surface, which does not occur on a regular spherical or ellipsoidal fcc particles or Wulff polyhedra. Another example is shown in Figure 4b. The pattern of the planar bulk defects, twin boundaries in this case, is reflected in changes of the surface faceting creating a local inward curvature of the particle. Despite the absence of stepped surface facets at this part of the particle, a number of steps are created by the inward kinks, where the twin boundaries meet the surface. Figure 4c shows that twin boundaries can create unique surface ensembles even if the Cu surface of a larger particle appears essentially flat. The change of the surface faceting from 111 to 100 is associated only with a slightly obtuse angle close to 180° . Neighboring to the position of the kink, a column of surface atoms is observed, whose position is sticking out of the regular surface (see arrow, Figure 4c, inset). Again, such arrangement can be described as a high energy site created by the termination of a planar defect at the surface of the Cu particle.

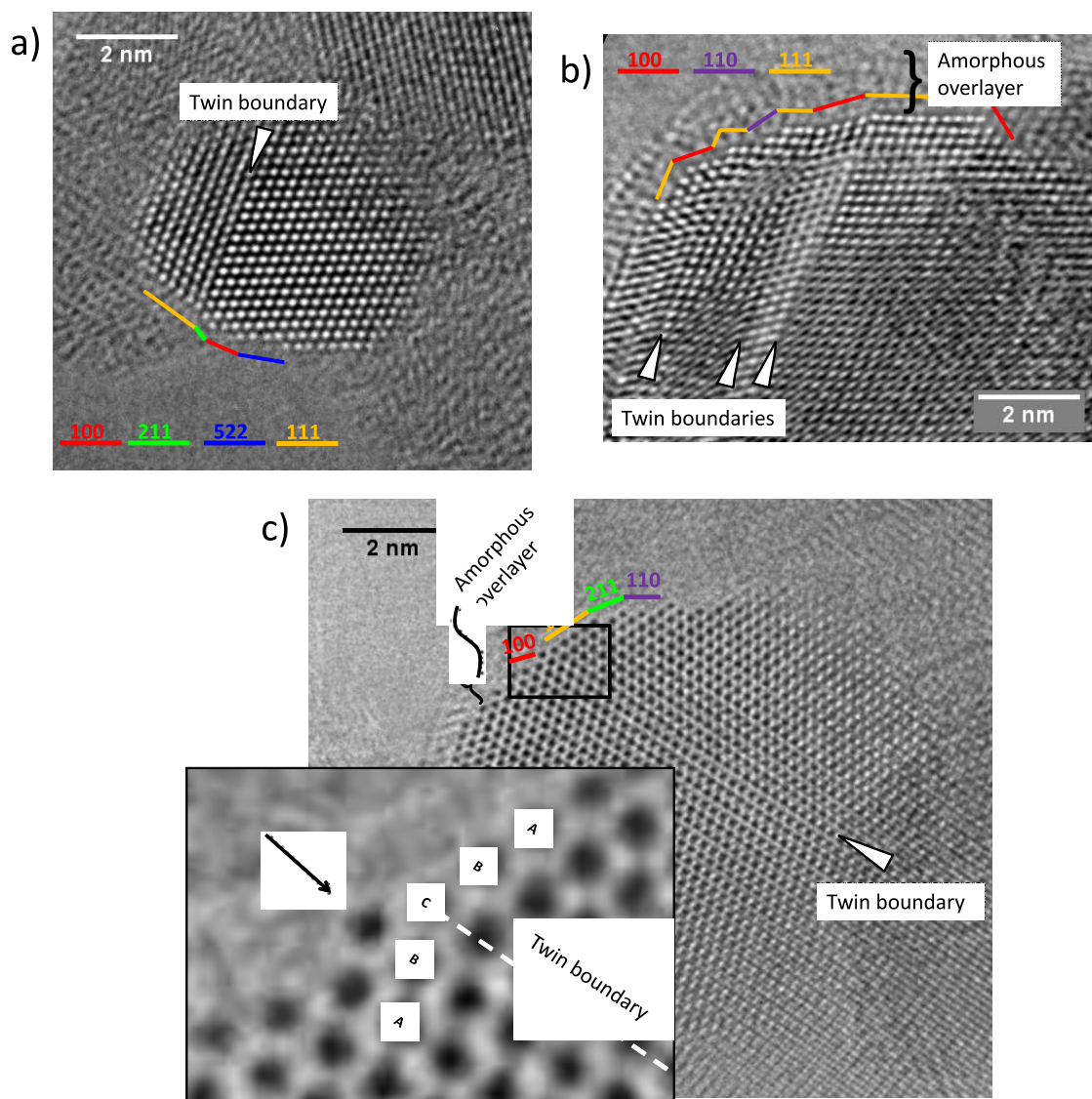


Figure 4: Aberration-corrected HRTEM images of Cu particles in the conventionally prepared, most active Cu/ZnO/Al₂O₃ catalyst.

As the presence of a defect at the active site alone does not directly involve ZnO, it cannot explain the observation^{33,34} of Cu-ZnO synergy in physical mixtures. It seems likely that the Cu-ZnO synergy is related to strong metal support interaction (SMSI) between Cu and ZnO leading to a partial coverage of the Cu surface with ZnO_x under reducing conditions. SMSI has been observed on Cu/ZnO-based catalysts using vibrational spectroscopy,³⁵ thermal desorption of probe molecules,³⁶ and by monitoring the wetting behavior of Cu/ZnO model catalysts.³⁷ In the high-performance catalyst studied here, the presence of an amorphous over-layer of the Cu particles with a thickness of approximately 1 nm can be seen in some HRTEM images (Figure 4b,c). In the complex real catalyst, fully covered particles coexist with partially covered and practically uncovered ones. To identify the layer as ZnO_x, we have investigated the surface composition of the most active catalyst using ambient X-ray photoemission spectroscopy (XPS). In agreement with literature data,³⁸⁻⁴¹ the Cu:Zn ratio at the catalyst's surface drops during activation in hydrogen. For our catalyst the Cu:Zn ratio is inverted from its nominal value of 70:30 (calcined) to ca. 30:70 (reduced), supporting the idea of an

SMSI effect (Figure 5a). The (partial) ZnO_x coverage of the surface of the reduced Cu particles in the catalyst was finally evidenced by tuning the information depth of the experiment from approximately ca. 0.6 to ca. 2.3 nm by variation of the kinetic energy of the incoming beam (Figure 5b). Core level fitting of the Zn 3p and Cu 3p signals show the enrichment of Zn at the surface of the catalyst (for details see supporting information), while with a higher information depth the Cu:Zn ratio is slowly approaching towards the nominal composition. The calcined catalyst does not show any surface enrichment of Zn and the effect is fully reversible upon re-calcination of the catalyst. Given the dynamics of the ZnO component in this Cu/ZnO catalyst and that the surface decoration of the Cu particles already at relatively mild conditions of low partial pressure of hydrogen, further progression of this effect under strongly reducing industrial methanol synthesis conditions may be envisioned leading to formation of a CuZn surface alloy as proposed by several authors.^{14,35,37}

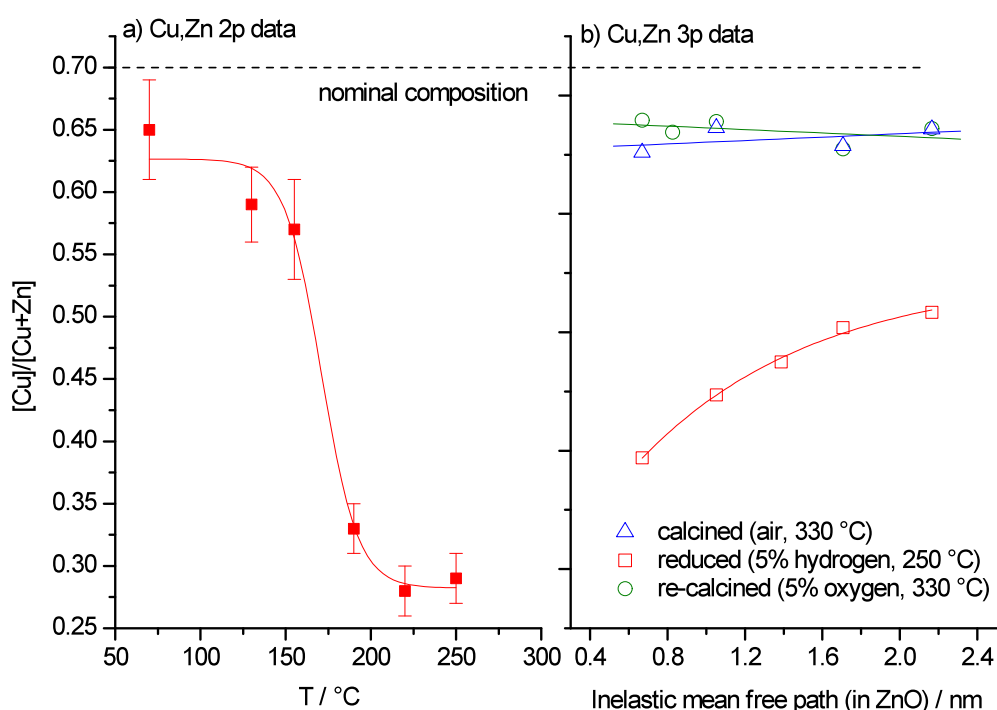


Figure 5: Surface and near-surface composition of the most active Cu/ZnO/Al₂O₃ catalyst of this study with a Cu:Zn ratio of 70:30 recorded with synchrotron XPS. a) in-situ Cu,Zn 2p data during reduction in 0.25 mbar hydrogen with a heating rate of 2 K/min. b) environmental Cu,Zn 3p data of the calcined, the pre-reduced (in 5% hydrogen at 250 °C) and re-calcined (5% oxygen at 330 °C) catalyst as a function of information depth. Lines are guides to the eye.

The beneficial role of Zn at the catalyst's surface can be explained by DFT calculations. To incorporate the effect of Zn, Cu(211) surfaces where Cu in the step is partially substituted by Zn was studied (Figure 3, red curves). Alloying of Zn into the Cu step does further increase the adsorption strength of HCO, H₂CO and H₃CO and decreases the barriers. Hence, the rate of methanol synthesis is further increased. The order of activity CO₂ as well as for CO hydrogenation is CuZn(211) > Cu(211) > Cu(111). The most active surface is therefore found to be a Cu step with Zn alloyed into it. The adsorption properties of alloyed CuZn(111) surface have been experimentally observed to be modified from those of pure Cu(111).⁴²

Combining the experimental and theoretical results, a model for the active site of methanol synthesis over industrial catalysts emerges. Undistorted pure Cu was found to be quite inactive in the methanol synthesis experiment. The same result was obtained for the flat Cu(111) surface in the DFT calculations. High activity was generated by two factors. Firstly, the presence steps at the Cu surface is required, which can be stabilized by bulk defects like stacking faults or twin boundaries terminating at the surface. The increase in activity is explained by a stronger binding of the intermediates on stepped sites and lower energy barriers between them. The bulk defect structure in the real catalyst is a result of a well-optimized low temperature preparation method. The second requirement is the presence of Zn at the defective (stepped) Cu surface, which in the high performance catalyst is a result of a dynamic SMSI effect leading to partial coverage of the metal particles with ZnO_x. Substitution of Zn into the Cu steps further strengthens the binding of the intermediates and increases the activity of the catalyst. The data presented suggest that the presence of steps and their close vicinity to ZnO_x on the surface of the Cu particles creates the ensemble needed to render the very active “methanol copper”, a Cu step with partial Zn alloying. These two requirements are fulfilled only for a small and varying fraction of the metallic Cu surface area explaining the differences in intrinsic activity observed in this study and in literature. Thus, under industrially relevant conditions a small fraction of the surface is largely contributing to the activity, which cannot be easily mimicked by simplified model approaches.

¹ www.methanol.org, Sept. 2010.

² G. A. Olah, A. Goepfert, G. K. Surya Prakash, *Beyond Oil and Gas: The Methanol Economy*, Wiley-VCH, Weinheim, 2006.

³ J. B. Hansen, P. E. Højlund Nielsen, *Methanol Synthesis in: Ertl G, Knözinger H, Schüth F, Weitkamp J (eds) Handbook of Heterogenous Catalysis, 2nd edn. Wiley-VCH, Weinheim (2008) 2920-2949.*

⁴ D. Waller, D. Stirling, F. S. Stone, M. S. Spencer, *Faraday Discuss. Chem. Soc.* 87 (1989) 107.

⁵ M. S. Spencer, *Top. Catal.* 8, (1999) 259-266.

⁶ I. Kasatkin, P. Kurr, B. Kniep, A Trunschke, R. Schlögl, *Angew. Chem.* 119 (2007) 7465.

⁷ M. Behrens; *J. Catal.* 267 (2009) 24-29.

⁸ M. Kurtz, H. Wilmer, T. Genger, O. Hinrichsen, M. Muhler, *Catal. Lett.* 86 (2003) 77.

⁹ The exposed Cu surface area can be measured using the N₂O chemisorption method, see, e.g., a) G. C. Chinchin, C. M. Hay, H. D. Vanderwell, K. C. Waugh, *J. Catal.* 103 (1987) 79., b) O. Hinrichsen, T. Genger, M. Muhler, *Chem. Eng. Technol.* 23 (2000) 956.

¹⁰ M. Kurtz, N. Bauer, C. Büscher, H. Wilmer, O. Hinrichsen, R. Becker, S. Rabe, K. Merz, M. Driess, R. A. Fischer, M. Muhler, *Catal. Lett.* 92 (2004) 49.

¹¹ Yoshihara, J., Campbell, C. T., *J. Catal.* 161 (1996) 776-781.

¹² P. B. Rasmussen, P. M. Holmblad, T. Askgaard, C. V. Oevesen, P. Stoltze, J. K. Nørskov, I. Chorkendorff, *Catal. Lett.* 26 (1994) 373-3881.

¹³ J. Szani, D. W. Goodman, *Catal. Lett.* 10 (1991) 383.

¹⁴ R. Burch, R. J. Chappell, S. E. Golunski, *J. Chem Soc. Faraday Trans.* 85 (1989), 3569.

¹⁵ Y. Kanai, T. Watanabe, T. Fujitani, T. Uchijima, J. Nakamura, *Catal. Today* 28 (1996) 223.

¹⁶ M. S. Spencer, *Top. Catal.* 8 (1999) 259-266.

¹⁷ K. Klier, *Adv. Catal.* 31 (1982) 243-313.

¹⁸ V. Ponc, *Surf. Sci.* 272 (1992) 111-117.

¹⁹ W.P.A. Jansen, J. Beckers, J.C. v. d. Heuvel, A.W. Denier v.d. Gon, A. Blik, and H.H. Brongersma, *J. Catal.* 210 (2002) 229-236.

²⁰ J.C. Frost, *Nature* 334 (1988) 577.

²¹ J. Nakamura, Y. Choi, T. Fujitani, *Top. Catal.* 22 (2003) 277-285.

²² K.C. Waugh, *Catal. Today* 15 (1992) 51-75.

²³ P. L. Hansen, J. B. Wagner, S. Helveg, J. R. Rostrup-Nielsen, B. S. Clausen, H. Topsøe, *Science* 295 (2002) 2053.

²⁴ P. C. K. Vesborg, I. Chorkendorff, I. Knudsen, O. Balmes, J. Nerlov, A. M. Molenbroek, B. S. Clausen, S. Helveg, *J. Catal.* 262 (2009) 65.

-
- ²⁵ M. M. Günter, T. Ressler, B. Bems, C. Büscher, T. Genger, O. Hinrichsen, M. Muhler, R. Schlögl, *Catal. Lett.* 71 (2001) 37.
- ²⁶ This effect is due to the generation of thin hexagonal domains in the cubic lattice with the change in stacking sequence of the hexagonally close packed (111) layers at the stacking fault (ideal A-B-C-A, stacking fault A-B-C-B-C-A, twin boundaries A-B-C-B-A). For more details and quantitative treatment see, e.g., ref. 27.
- ²⁷ Warren, B.E., *X-ray Diffraction* (New York: Dover Publications), 1990
- ²⁸ Experimental results suggest that CO₂ is the major carbon source for methanol at low conversions, see, e.g., Chinchin, G.C., Denny, P.J., Jennings, J.R., Spencer, M.S., Waugh, K.C., *Appl. Catal.* 36 (1988) 1-65.
- ²⁹ L. C. Grabow, M. Mavrikakis, *ACS Catal.* 1 (2011), 365.
- ³⁰ Z.-M. Hu, K. Takahashi, H. Nakatsuji, *Surf. Sci.* 442 (1999), 90.
- ³¹ Y. Yang, J. Evans, J. A. Rodriguez, M. G. White, P. Liu, *Phys. Chem. Chem. Phys.* 12 (2010), 9909.
- ³² Y. Morikawa, K. Iwata, K. Terakura, *Appl. Surf. Sci.* 169-170 (2001), 11.
- ³³ J. Nakamura, T. Uchijima, Y. Kanai, T. Fujitani, *Catal. Today* 28 (1996) 223-230.
- ³⁴ R. Burch, S. E. Golunski, M. S. Spencer, *J. Chem. Soc., Faraday Trans* 28 (1990) 2683.
- ³⁵ N.-Y. Topsøe, H. Topsøe, *Top. Catal.* 8 (1999) 267.
- ³⁶ R. Naumann d'Alnoncourt, X. Xia, J. Strunk, E. Löffler, O. Hinrichsen, M. Muhler, *Phys. Chem. Chem. Phys.* 13 (2006) 1525
- ³⁷ J. D. Grunwaldt, A. M. Molenbroek, N. Y. Topsoe, H. Topsoe, B. S. Clausen, *J. Catal.* 194 (2000) 452.
- ³⁸ J. Słoczyński, R. Grabowski, P. Olszewski, A. Kozłowska, J. Stoch, M. Lachowska, J. Skrzypek, *Applied Catalysis A: General* 310 (2006) 127–137.
- ³⁹ Raimondi et al., *Appl. Surf. Sci.* 189 (2002) 59.
- ⁴⁰ Petrini, Garbassi, *J. Catal.* 90 (1984) 113.
- ⁴¹ Goodby, Pemberton, *Appl. Spectros.* 42 (1988) 754.
- ⁴² J. Nakamura, Y. Choi, T. Fujitani, *Top. Catal.* 22 (2003) 277.

Acknowledgement:

The authors thank Martin Muhler (Ruhr-University Bochum, Germany) and Olaf Hinrichsen (Technical University Munich, Germany) for fruitful discussions. The Bundesministerium für Bildung und Forschung (FKZ 01RI0529, 2005-2008) and the Bayerisches Wissenschaftsministerium (NW-0810-0002, since 2010) is acknowledged for financial support of this work. F.S., F.A.-P., and J.K.N. wish to acknowledge support from the (U.S.) Department of Energy (DOE), Office of Basic Energy Sciences.